Energy Proceedings
Vol 41, 2024
ISSN 2004-2965

Performance Analysis of a Counter-flow Cooling Tower Under Different Weather Conditions

Abdulsalam M.A. Hasan[1], Esmail M.A. Mokheimer[1,2,3,*]

1 Mechanical Engineering Department, King Fahd University of Petroleum & Minerals, Dhahran, Saudi Arabia

2 Interdisciplinary Research Center for Renewable Energy and Power Systems (IRC-REPS), King Fahd University of Petroleum & Minerals, Dhahran, Saudi Arabia

3 K.A. CARE Energy Research and Innovation Center, Dhahran, Saudi Arabia
(*Corresponding Author: esmailm@kfupm.edu.sa)

ABSTRACT

The performance of the cooling tower is profoundly influenced by the climatic conditions. This study examines cooling tower performance in 42 diverse Saudi Arabian cities, addressing gaps in existing literature considering the performance parameters of temperature range, and cooling capacity. To assess the performance of the cooling tower, a mathematical model is developed and solved using the Engineering Equation Solver (EES). The assessment of the cooling tower's performance is conducted with a focus on yearly and monthly average dry-bulb temperatures as well as relative humidity. Based on the yearly average weather data, the cooling tower in Jazan exhibits the lowest performance with a temperature range of 4°C and a 50-kW cooling capacity. In Abha, the cooling tower demonstrates the best performance despite different weather conditions with almost a 7.61°C range and 95.4-kW cooling capacity. Evaluating the monthly average weather data, the cooling tower in Abha excels compared to the cooling tower in the other cities, achieving a cooling capacity of 86.1-kW in August outperforming its counterpart in Jazan by 53.5%. The summer weather conditions in Abha have led to a slight reduction in the cooling capacity of only 16.3% in comparison to the cooling capacity in winter (January).

Keywords: cooling tower performance, cooling capacity, temperature range, wet-bulb temperature, dry bulb-temperature, relative humidity

NONMENCLATURE

Symbols

A	Surface Area, (m^2)
A_V	Water Droplets Area Per Unit Volume, $\left(\frac{m^2}{m^3}\right)$
C_{Pa}	Air Specific Heat at Constant Pressure, $\left(\frac{kJ}{kg.℃}\right)$
C_{Pw}	Water Specific Heat at Constant Pressure, $\left(\frac{kJ}{kg.℃}\right)$
h	Specific Enthalpy, $\left(\frac{kJ}{kg}\right)$
h_c	Heat Transfer Coefficient, $\left(\frac{kW}{m^2.K}\right)$
h_D	Mass Transfer Coefficient, $\left(\frac{kg_w}{m^2.s}\right)$
$h_{fg,w}$	Latent Heat of Vaporization, $\left(\frac{kJ}{kg}\right)$
h_g^0	Saturated Water Vapor Specific Enthalpy at Zero ℃, $\left(\frac{kJ}{kg}\right)$
$\dot{m}_a$	Air Mass flowrate, $\left(\frac{kg}{s}\right)$
$\dot{m}_w$	Cooling Water Mass flowrate, $\left(\frac{kg}{s}\right)$
P	Pressure, (kPa)
$\dot{Q}$	Rate of Heat Transfer, (kW)
ρ	Density, $\left(\frac{kg}{m^3}\right)$
T	Temperature, $(℃)$
U	Overall Heat Transfer Coefficient, $\left(\frac{kW}{m^2.K}\right)$
V	Volume, (m^3)
W	Humidity Ratio, $\left(\frac{kg_w}{kg_a}\right)$

This is a paper for 15th International Conference on Applied Energy (ICAE2023), Dec. 3-7, 2023, Doha, Qatar.

1. INTRODUCTION

Cooling towers play a crucial role in various applications, including vapor compression chillers [1], adsorption chillers [2], absorption chillers [3], and power plants [4] (see Fig. 1). These towers consist of three main zones: the rain zone, the spray zone, and the packing. The rain and spray zones facilitate water-air contact through droplet formation, while the packing provides an extended contact area [5]. In vapor compression chillers, cooling towers cool the condenser water and dissipate heat from the cycle. They achieve this by circulating water through nozzles that uniformly distribute it over the packing fill, promoting evaporation. Makeup water compensates for evaporated water, resulting in cold water exiting the tower and warm, moist air [6].

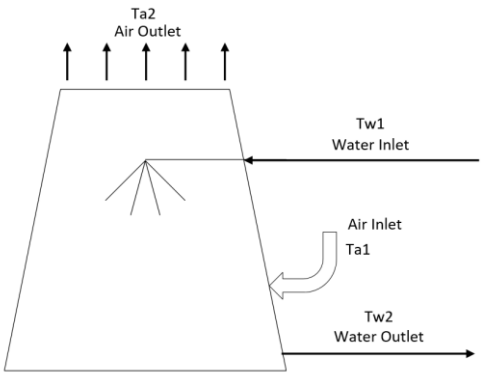

Fig. 1. Counter-Flow Cooling Tower Schematic Diagram

Numerous studies have focused on optimizing cooling tower performance. Cui et al. [7] optimized tower operation by considering droplet size and gas velocity effects. Li et al. [8] explored water distribution's impact on cooling tower performance. Singh and Das [9] proposed a feedback model for performance prediction. Alazazmeh et al. [10] introduced an innovative air-cooling system. Pandelidis et al. [11] investigated the Maisotsenko cooling tower's unique capabilities. It has been proven that the Maisotsenko cooling tower could decrease the temperature of the water to be less than the wet-bulb temperature even in highly hot and humid conditions, which is not achievable with traditional cooling towers.

Several publications studied factors like packing fill fouling and material type [5], [12]–[19]. Khan et al. [12] evaluated counter flow wet cooling towers' performance, noting the impact of fouling. Yu et al. [5] developed a model for heat exchange in packing fill. According to the results, the cooling tower's output water temperature rises when air humidity rises, but a smaller droplet radius and greater flow rate ratio result in a lower temperature of the outlet water and better cooling tower performance. Amini et al. [13] observed improved performance using nanofluids. Lavasani et al. [14] examined packing rotation's effects. Lyu et al. [15] explored different packing designs. Rahmati et al. [16] studied film packing's impact. Tomás et al. [17] investigated alternative materials. Lucas et al. [18], [20] studied how the performance of the cooling tower was affected using six different types of drift eliminators in an effort to reduce the amount of water loss. Shahali et al. [19] improved cooling tower conditions with different packing rib counts.

Additionally, some studies analyzed natural draft cooling towers and crosswind effects [21]–[25]. Wei et al. [21] examined crosswind effects on cooling towers. Their findings showed that wind reduces the performance of cooling towers. Zhai and Fu [22] used windbreak walls to mitigate crosswind effects. The outcomes demonstrated that the outside windbreak wall can successfully minimize the crosswind's detrimental effects. Sun et al. [23] studied air-directing impact channels. The findings indicated how these channels can improve performance in crosswind conditions by boosting the air flowrate inside the cooling tower. Gao et al. [24] analyzed high-level water-collecting towers in crosswind conditions. According to the study, when crosswind velocity rises, the effects of crosswinds on performance and the temperature distribution for the air within the tower get worse. Chen et al. [25] enhanced cooling tower performance using air ducts in the rain region. Their research showed that using the ducts of the air improved the cooling tower performance, where the improvement depends on the crosswind velocity.

This study assesses and compares cooling tower performance across various Saudi Arabian cities, considering diverse climate conditions and diurnal variations. We develop a mathematical model, solve it using EES, and aim to identify the city with the best cooling tower performance, highlighting influential factors. This research addresses a gap in the existing literature by examining cooling tower performance in different Saudi Arabian cities.

2. MATHEMATICAL MODEL

The main assumptions that used to the development of the modelling equations can be given as follow [26]:

1. Mass transfer and heat transfer through the walls of the cooling tower to the environment can be neglected.

2. Mass transfer and heat transfer coefficient can be assumed to be constant.
3. The heat transfer from the fan motor to the water or the air can be neglected.
4. The specific heats of the water and the air can be assumed to be constant.
5. Lewis number value can be assumed to be constant and unity.
6. The cross-sectional area of the cooling tower can be assumed to be uniform.
7. The water temperature is assumed to be uniform.

Fig. 2 illustrates the cooling tower mass and energy analysis at the whole tower and at the differential volume.

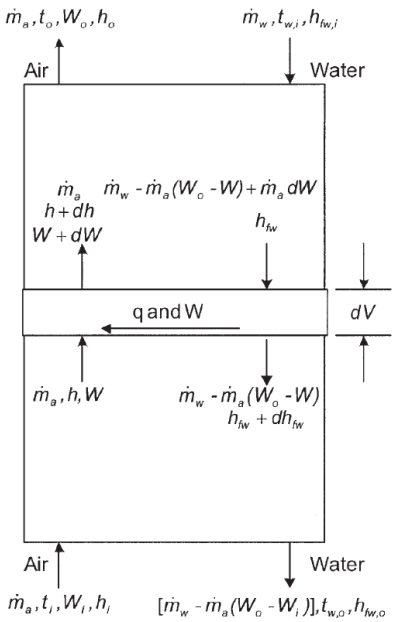

Fig. 2. The Cooling Tower Mass and Energy Balance [12]

2.1 Mass Balance at the Entire System

$$\dot{m}_a W_o + \dot{m}_{wo} = \dot{m}_a W_i + \dot{m}_w \quad (1)$$

After rearranging the above balance, the mass flowrate at the exit of the cooling tower $(\dot{m}_{wo})$ will be as follows:

$$\dot{m}_{wo} = \dot{m}_w - \dot{m}_a(W_o - W_i) \quad (2)$$

Following the previous equation, if the W is located at any point inside the cooling tower, the mass flowrate of the water at the exit of the differential volume (DV) $(\dot{m}_{wo,DV})$ can be defined as follows:

$$\dot{m}_{wo,DV} = \dot{m}_w - \dot{m}_a(W_o - W) \quad (3)$$

2.2 Mass Balance at the Differential Volume

$$\dot{m}_a w + \dot{m}_{wi,DV} = \dot{m}_a(w + dw) + \dot{m}_{wo,DV} \quad (4)$$

Replace $\dot{m}_{wo,DV}$ in eq. (4) using eq. (3)

$$\dot{m}_a w + \dot{m}_{wi,dv} = \dot{m}_a(w + dw) + [\dot{m}_w - \dot{m}_a(w_o - w)] \quad (5)$$

After rearranging the above balance, the mass flowrate at the inlet of the DV $(\dot{m}_{wi,DV})$ will be as follows:

$$\dot{m}_{wi,dv} = \dot{m}_w - \dot{m}_a(w_o - w) + \dot{m}_a dw \quad (6)$$

Where $(\dot{m}_a dw)$ means that before the DV, the $\dot{m}_w$ was greater than after it by almost $\dot{m}_a dw$.

2.3 Energy Balance at the Entire System

$$\dot{m}_a h_o + h_{fwo}[\dot{m}_w - \dot{m}_a(w_o - w_i)] = \dot{m}_a h_i + \dot{m}_w h_{fwi} \quad (7)$$

Rearranging the previous balance:

$$\dot{m}_a = \frac{\dot{m}_w(h_{fwi} - h_{fwo})}{[h_o - h_i - h_{fwo}(w_o - w_i)]} \quad (8)$$

2.4 Energy Balance at the Differential Volume

The following balance can be obtained using steady-state mass and energy balances on a DV:

$$\dot{m}_a(h + dh) + (h_{fw} + dh_{fw})[\dot{m}_w - \dot{m}_a(w_o - w)] = \dot{m}_a h + h_{fw}[\dot{m}_w - \dot{m}_a(w_o - w) + \dot{m}_a dw] \quad (9)$$

Rearranging eq. (9):

$$\dot{m}_a dh = -\big(\dot{m}_w - \dot{m}_a(W_o - W)\big)dh_{f,w} + \dot{m}_a dW h_{f,w} \quad (10)$$

Where $\big(\big(\dot{m}_a(W_o - W)\big)dh_{f,w}\big)$ is a very small amount and can be neglected. Moreover, the above equation becomes as follows:

$$\dot{m}_a dh = -\dot{m}_w dh_{f,w} + h_{fw}\dot{m}_a dw \quad (11)$$

The first term in the previous equation can be written using the mass and heat transfer coefficients (h_D, h_c), as follows:

$$-\dot{m}_w dh_{fw} = h_c A_V dV(T_w - T) + \dot{m}_a dw h_{fg,w} \quad (12)$$

$$-\dot{m}_w dh_{f,w} = h_c A_V dV(T_w - T) + h_D A_V dV\big(W_{s,w} - W\big)h_{fg,w} \quad (13)$$

The following equation represents the amount of water vapor in the air side:

$$d\dot{m}_w = \dot{m}_a dW = h_D A_V dV\big(W_{s,w} - W\big) \quad (14)$$

The ratio of the Schmidt number (Sc) to the Prandtl number (Pr) represents the Lewis number (Le):

$$\mathrm{Le} = \frac{\mathrm{Sc}}{\mathrm{Pr}} \quad (15)$$

$$\mathrm{Sc} = \frac{\nu}{D} \quad (16)$$

$$\mathrm{Pr} = \frac{\nu}{\alpha} \quad (17)$$

The previous form of the Le number is available in the literature, but researchers prefer to use the following Le by substituting the Sc and Pr ratios in the previous Le:

$$Le = \frac{h_c}{h_D C_{pa}} \quad (18)$$

Lewis number can be substituting in equation (13) to get the following simplified equation:

$$-\dot{m}_w dh_{f,w} = h_D A_V dV\left(LeC_{pa}(T_w - T) + (W_{s,w} - W)h_{fg,w}\right) \quad (19)$$

The following equation represents the approximation of constant C_{Pa}:

$$(h_{sw} - h) = C_{Pa}(T_w - T) + h_g^0(W_{ws} - W) \quad (20)$$

After combining equations (11), (14), (19), and (20) and simplified them, the following equation can be obtained:

$$\frac{dh}{dW} = Le\left(\frac{h_{s,w} - h}{W_{s,w} - W}\right) + (h_{g,w} - h_g^0 Le) \quad (21)$$

Eq. (21) describes the psychrometric chart condition line. The program is designed to solve first-order differential equations. It accomplishes this by integrating both sides of the equation to transform it into an appropriate form, which is then solved using EES for initial value problems. It's important to note that integration is performed in a specific direction, from the bottom to the top, which is similar to that described in Khan et al. [12]. By following this process, the program can efficiently and accurately solve differential equations.

2.5 Integral Forms

The pertinent equations from (22) to (25) are expressed in the following manner [27]:

$$W = W_i + \int_{V_i}^{V}\left(\frac{dW}{dV}\right)dV \quad (22)$$

$$\dot{m}_w = \dot{m}_{w,o} + \int_{V_i}^{V}\left(\frac{d\dot{m}_w}{dV}\right)dV \quad (23)$$

$$h = h_i + \int_{V_i}^{V}\left(\frac{dh}{dV}\right)dV \quad (24)$$

$$T_w = T_{w,o} + \int_{V_i}^{V}\left(\frac{dT_w}{dV}\right)dV \quad (25)$$

To clarify, 'V_i' can be taken zero and the terms in brackets on the right-hand side of equations (22) to (25) can be obtained as follows:

These terms $\left(\frac{dW}{dV}\right), \left(\frac{d\dot{m}_w}{dV}\right)$ can be replaced by rearranging eq. (14) as follows:

$$\frac{dw}{dV} = \frac{1}{\dot{m}_a} h_D A_V (W_{sw} - W) \quad (26)$$

$$\frac{d\dot{m}_w}{dV} = h_D A_V (W_{sw} - W) \quad (27)$$

After combining eq's. (21) and (26), the following term can be obtained $\left(\frac{dh}{dV}\right)$:

$$\frac{dh}{dV} = \left(\frac{h_D A_V}{\dot{m}_a}\right)\left[Le(h_{s,w} - h) + (h_{g,w} - h_g^0 Le)(W_{sw} - W)\right] \quad (28)$$

After replacing this term dh_{fw} in eq. (11) to $dt_w C_{Pw}$ and combining it with eq's. (26) and (28) the following term can be obtained $\left(\frac{dT_w}{dV}\right)$:

$$\frac{dT_w}{dV} = \frac{(W_{sw} - W)h_D A_V}{C_{Pw}\dot{m}_w}\left[\frac{Le(h_{s,w} - h)}{(W_{sw} - W)} + (h_{g,w} - h_g^0 Le) - h_{fw}\right] \quad (29)$$

2.6 Design and Performance Parameters

If $h_D A_V$ value is known, the appropriate cooling tower volume can be calculated using the following equation:

$$V = \frac{\dot{m}_a}{h_D A_V}\int_{W_i}^{W_o}\frac{dW}{W_{s,w} - W} \quad (30)$$

The number of transfer units can be estimated by using the following equation:

$$NTU_{cal} = \frac{h_D A_V V}{\dot{m}_a} = \int_{W_i}^{W_o}\frac{dW}{W_{s,w} - W} \quad (31)$$

The cooling tower characteristics can be estimated using the following equation:

$$Ka = \frac{h_D A_V V}{\dot{m}_w} \quad (32)$$

The effectiveness of the cooling tower is the ratio of the actual energy over the maximum possible energy and can be calculated by using the following equation:

$$\varepsilon = \frac{\text{Range}}{\text{Max. Range}} = \frac{\text{Range}}{\text{Range} + \text{Approach}} \quad (33)$$

$$\varepsilon = \frac{h_o - h_i}{h_{s,w,i} - h_i} \quad (34)$$

$$\text{Range} = T_{w,i} - T_{w,o} \quad (35)$$

$$\text{Approach} = T_{w,o} - T_{wb,i} \quad (36)$$

The conventional effectiveness equation used to evaluate cooling tower performance can be misleading, especially in hot and humid conditions. In such environments, the effectiveness value tends to increase, which may not accurately reflect the cooling tower's actual performance. This increase in effectiveness is primarily due to the water outlet temperature being closer to the inlet water temperature, resulting in a lower temperature range. Additionally, the wet bulb temperature, being close to the inlet water temperature, further reduces the maximum range achievable in these conditions. As a result, the difference between the actual temperature range and the maximum possible range decreases, leading to an apparent increase in the effectiveness value. To overcome this limitation and obtain a more comprehensive assessment of the cooling tower's efficiency, another parameter called the cooling capacity has been introduced. The cooling capacity takes into account both the water mass flow rate and the temperature range, providing a more meaningful and accurate representation of the cooling tower's

performance. The cooling capacity can be expressed using the following equation:

$$\dot{Q}_{CC} = \dot{m}_w C_P (\text{Range}) \quad (37)$$

2.7 Methodology

The mathematical model utilized in this study is solved using the Engineering Equation Solver (EES) software. Notably, the cooling tower is operated with a hot water entering from the top and cold air entering from the bottom. Thus, the integration process proceeds

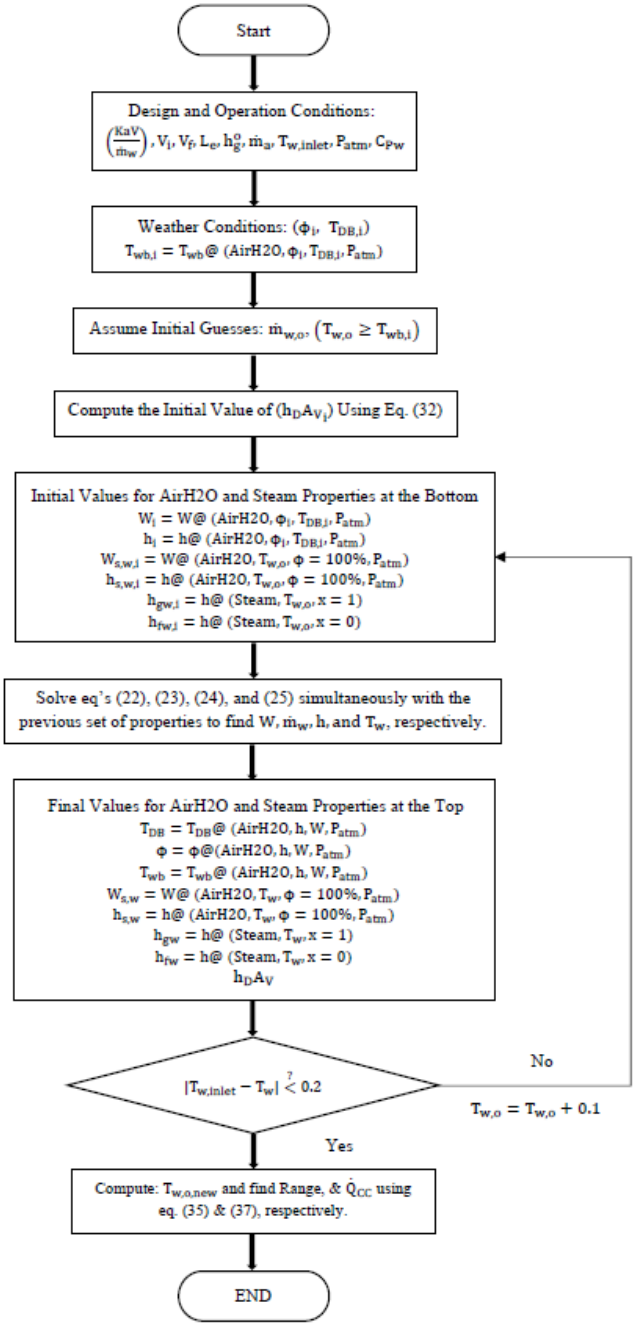

Fig. 3. Cooling Tower Mathematical Model Solution Procedure Flowchart

from the bottom to the top, or vice versa, to simulate the flow of fluids within the tower. To initiate the integration, initial values for the water temperature and water flow rate are assumed at the bottom of the tower. The predicted water temperature at the top is then iteratively compared with the desired value, and if not reached, a new assumed value is assigned to the water temperature at the bottom. This iterative process is facilitated using a while loop, referred to as a Repeat command in the EES. The sequential steps for solving the mathematical model are depicted in Fig. 3.

2.8 *The Solution Algorithm and Flow Chart*

Fig. 3 illustrates the cooling tower mathematical model solution procedure flowchart.

3. VALIDATION

The validation of the cooling tower model is presented in this section in order to evaluate the validity of the model results by matching their compatibility with the experimental results in the literature. The validation is done two times, the first time with the experimental results of Lucas et al. [20], and the second time with the manufacturer's catalogue. EES is used for this purpose, and it runs under the idea that there must be an equal number of variables and equations to solve simultaneous equations.

The experimental data reported by Lucas et al. [20] are used to validate the current model using the design and operating conditions in Table 1.

Table 1 Design and Operating Conditions for the First Validation

V_i	0, (m^3)
V_f	0.873, (m^3)
h_g^o	2501, $\left(\frac{kJ}{kg}\right)$
L_e	1
C_P	4.18, $\left(\frac{kJ}{kg.k}\right)$
P_{atm}	101.325, (kPa)

Table 2 Model Validation Results with Lucas et al. [20]

ϕ (%)	$T_{db,i}$ (°C)	$T_{w,i}$ (°C)	$\dot{m}_{w,i}$ ($kg\ s^{-1}$)	$\dot{m}_a$ ($kg\ s^{-1}$)	$\frac{KaV}{\dot{m}_{w,i}}$	$T_{w,o}^{exp}$ (°C), [20]	$T_{w,o}$ (°C) For the Current Model	|Deviation| (%)
41.56	31.38	39.15	1.46	0.597	0.386	34.28	33.03	3.658
68.66	23.73	41.23	0.842	0.581	0.506	33.35	33.67	0.9565
67.06	23.39	38.48	1.139	0.588	0.454	32.59	31.84	2.307
32.66	31.46	35.29	1.402	0.935	0.472	30.35	29.02	4.37
60.85	24.76	35.77	1.131	0.965	0.559	29.75	28.94	2.726
66.84	24.47	37.64	0.844	0.922	0.688	29.74	30.03	0.9717

The validation results are listed Table 2. Table 2 shows that the current model results and the experimental data have an acceptable average deviation. These minor variations demonstrate that the current model is valid and dependable.

Now, the correlation in Table A1 is used to be validated with the current model. This correlation is made by using linear regression for an experimental data from the manufacturer's catalog, taking into account the range of each parameter in the Table A1. Table 3 shows the operating and design conditions taken from the catalog.

Table 3 Design and Operating Conditions for the Second Validation

V_i	0, (m^3)
V_f	1.789, (m^3)
$\dot{m}_{w,i}$	3, $\left(\frac{kg}{s}\right)$
$\dot{V}_a$	4600, $\left(\frac{m^3}{hr}\right)$
$\frac{KaV}{\dot{m}_{w,i}}$	0.5
h_g^o	2501, $\left(\frac{kJ}{kg}\right)$
L_e	1
C_P	4.18, $\left(\frac{kJ}{kg.k}\right)$
P_{atm}	101.325, (kPa)
$T_{w,i}$	35, $(°C)$

Table 4 shows the results of the comparison with the data from the catalog so that the comparison is made for the outlet water temperature. It turns out that the average deviation between the catalog data and the model results is relatively small and acceptable. Also, each parameter value is within the range specified in Table A1.

Table 4 The Validation Results with the Catalog Experimental Data

ϕ (%)	$T_{db,i}$ (°C)	$T_{w,o}^{exp}$ (°C)	$T_{w,o}$ (°C)	|Deviation| (%)	Q_{CC} (kW)
86.02	23.3	28.03	29.66	5.837	66.91
83.43	24	28.18	29.8	5.749	65.26
81.23	24.7	28.35	29.87	5.333	64.39
76.66	25.8	28.51	30.06	5.443	61.96
79.03	25.5	28.54	30.01	5.149	62.52

4. RESULTS AND DISCUSSION

In this section, a comprehensive analysis and discussion of the cooling tower's performance are presented. Temperature range and cooling capacity stand as performance parameters, their evaluation contingent upon the different weather conditions across different Saudi Arabian cities. Both monthly and yearly average weather data are considered as the foundation for evaluating the cooling tower's performance. A fundamental assumption is established regarding a constant inlet water temperature of 35°C for the cooling tower across all cities. This forms the basis for evaluating cooling tower performance and identifying the specific city with the most effective cooling, where the exiting water temperature is lower, thus signifying a greater cooling capacity.

4.1 The Impact of Yearly Average Weather Conditions on the Cooling Tower Performance

In this subsection, the results of the impact of yearly average weather conditions on various performance parameters are presented and explained. In order to conduct this study, the operating and design conditions that are provided by the manufacturer's catalog for a specific model of the cooling tower are utilized, which have been previously used in the validation section. To provide a comprehensive overview, Fig. 4 shows the behavior of yearly average dry-bulb and wet-bulb temperatures, along with changes in average yearly relative humidity. Each city exhibits distinct variations in

average temperatures and relative humidity, which directly impact the performance parameters of the cooling tower. The forthcoming sections will delve deeper into studying the consequences of these climate variations on the cooling tower performance.

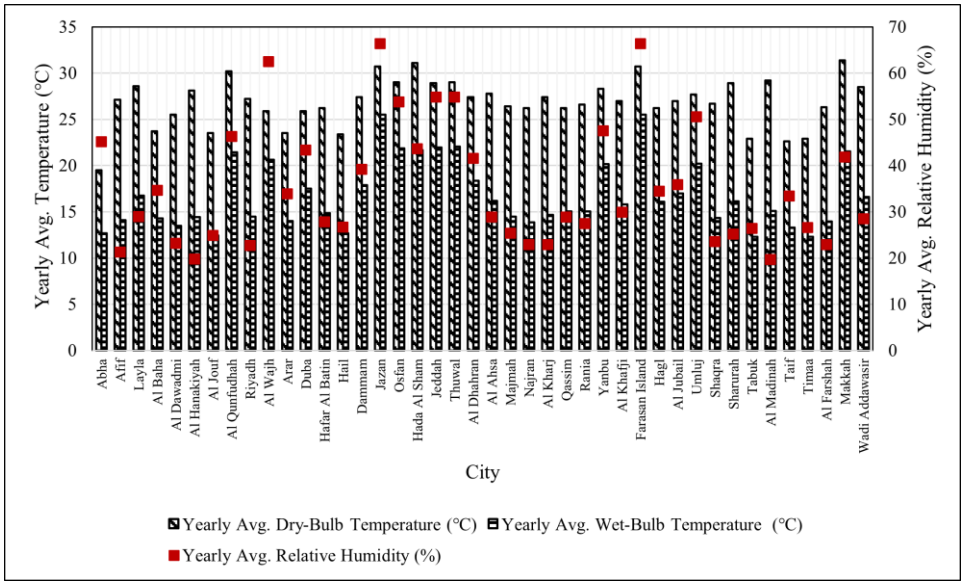

Fig. 4. Yearly Average Dry-Bulb Temperature, Wet-Bulb Temperature and Relative Humidity for 42 Cities in KSA

Fig. 5 illustrates the influence of yearly average climates on the range between inlet and outlet water temperatures. Notably, the most substantial temperature range, reaching 7.676°C, is observed in the cooling towers of Abha and Tabuk, whereas Jazan's cooling tower experiences a lower range of 3.978°C. This discrepancy arises primarily from variations in weather conditions, particularly the yearly average wet-bulb temperature. The optimal cooling tower operation aims to lower the outlet water temperature to its minimal value, equivalent to the wet-bulb temperature. In this context, Abha and Tabuk weathers exhibit relatively low wet-bulb temperatures, contributing to their higher temperature ranges, whereas Jazan's higher wet-bulb temperature influences cooling tower performance, leading to a lower temperature range. Noteworthy is the cooling tower in Al-Hanakiyah, presenting a range of 7.16°C, moderately average compared to other cities, which can be attributed to its average wet-bulb temperature.

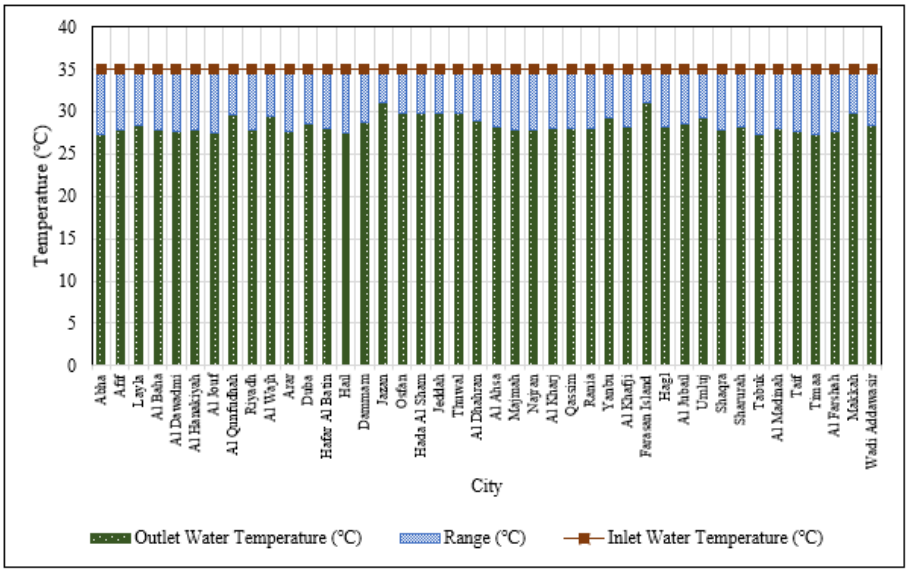

Fig. 5. The Impact of Various Yearly Average Weather Conditions on the Water Temperature Range of the Cooling Tower

Fig. 6 illustrates the impact of diverse yearly average weather conditions on the cooling capacity of cooling towers across all cities. Notably, the cooling tower in Abha and Tabuk achieves the highest cooling capacity at 96.26 kW, while the cooling tower in Jazan records the lowest cooling capacity at 49.88 kW. Importantly, the temperature range, influenced by varying weather conditions, significantly affects the cooling capacity, with the cooling tower in Jazan exhibiting a minimized range due to elevated wet-bulb temperatures, leading to a diminished cooling capacity. Additionally, the cooling tower in Al-Hanakiyah demonstrates an intermediate cooling capacity of 89.78 kW, reflecting its average standing in comparison to other cities, influenced by the average temperature range of the cooling tower in this city.

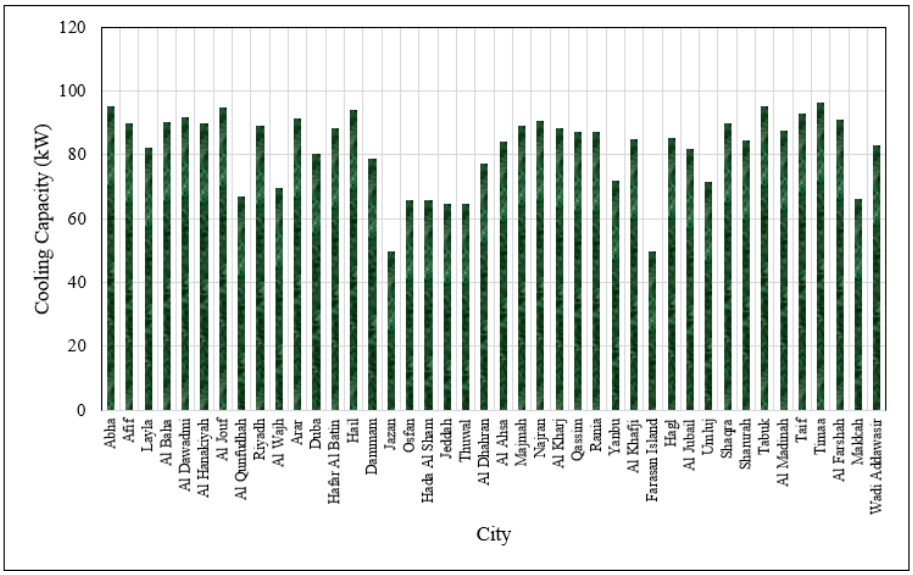

Fig. 6. The Impact of Various Yearly Average Weather Conditions on the Cooling Capacity of the Cooling Tower

4.2 The Impact of Monthly Average Weather Conditions on the Cooling Tower Performance in a Specific Cities

In this subsection, the results of the impact of monthly average weather conditions on various performance parameters are presented and explained. Specifically, our comprehensive analysis focuses on four cities: Abha, Jazan, Al-Hanakiyah, and Tabuk, as we delve into the cooling tower's performance across the entirety of the year on a monthly basis. Fig. 7 depicts the fluctuations in monthly average dry-bulb temperature, wet-bulb temperature, and relative humidity throughout the year within these four cities in the Kingdom. The figure illustrates the winter and summer weather conditions, highlighting a notably cold trend in the monthly average weather conditions in the winter, particularly evident in the wet-bulb temperatures. In January, all cities experience impressively low monthly average wet-bulb temperatures. During the summer months, a different pattern emerges. In June, Jazan and Al-Hanakiyah exhibit the highest monthly average wet-bulb temperatures, while in Abha and Tabuk, the highest monthly average wet-bulb temperatures are in August.

Fig. 8 illustrates the influence of monthly average climates on the range between inlet and outlet water temperatures in the same four cities. During the winter season, the cooling tower temperature range in Abha, Jazan, Al-Hanakiya, and Tabuk exhibits its highest range, notably pronounced in January, with readings of 8.208°C, 5.144°C, 8.281°C, and 8.999°C respectively. Transitioning to the summer months, different variations emerge. In Abha and Tabuk, the cooling tower range reaches its lowest point in August, measuring 6.866°C and 6.386°C respectively, while, for the cooling tower in Jazan and Al-Hanakiyah, the lowest temperature range in June, registering at 3.195°C and 5.869°C respectively. This trend mirrors the influence of monthly average wet-bulb temperatures, as evident in Fig. 7. This indicates that the cooling tower exhibits a superior temperature range in Abha's warmer months compared to other cities, particularly Jazan. Notably, the cooling tower's temperature range is at its lowest in Jazan during summer, emphasizing Abha's cooling tower advantage. This temperature range discrepancy underscores Abha's cooling tower superiority by a substantial 53.5% compared to the cooling tower temperature range in Jazan.

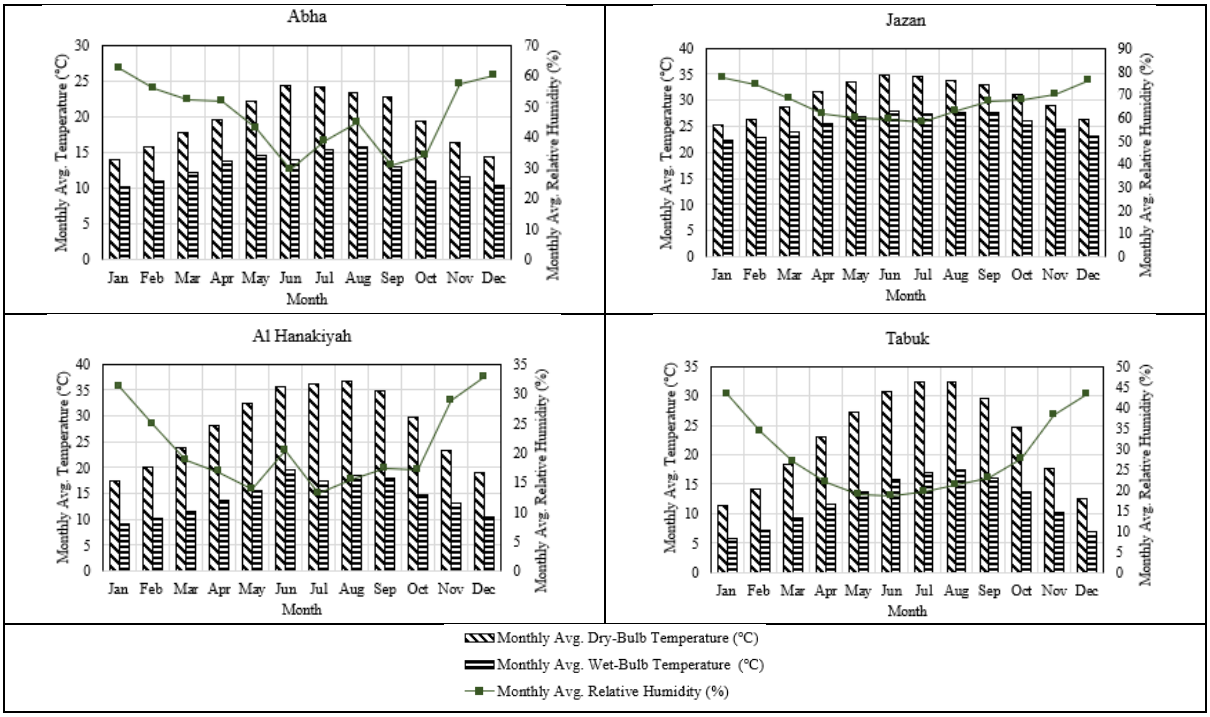

Fig. 7. Monthly Average Dry-Bulb Temperature, Wet-Bulb Temperature and Relative Humidity for 4 Cities in KSA

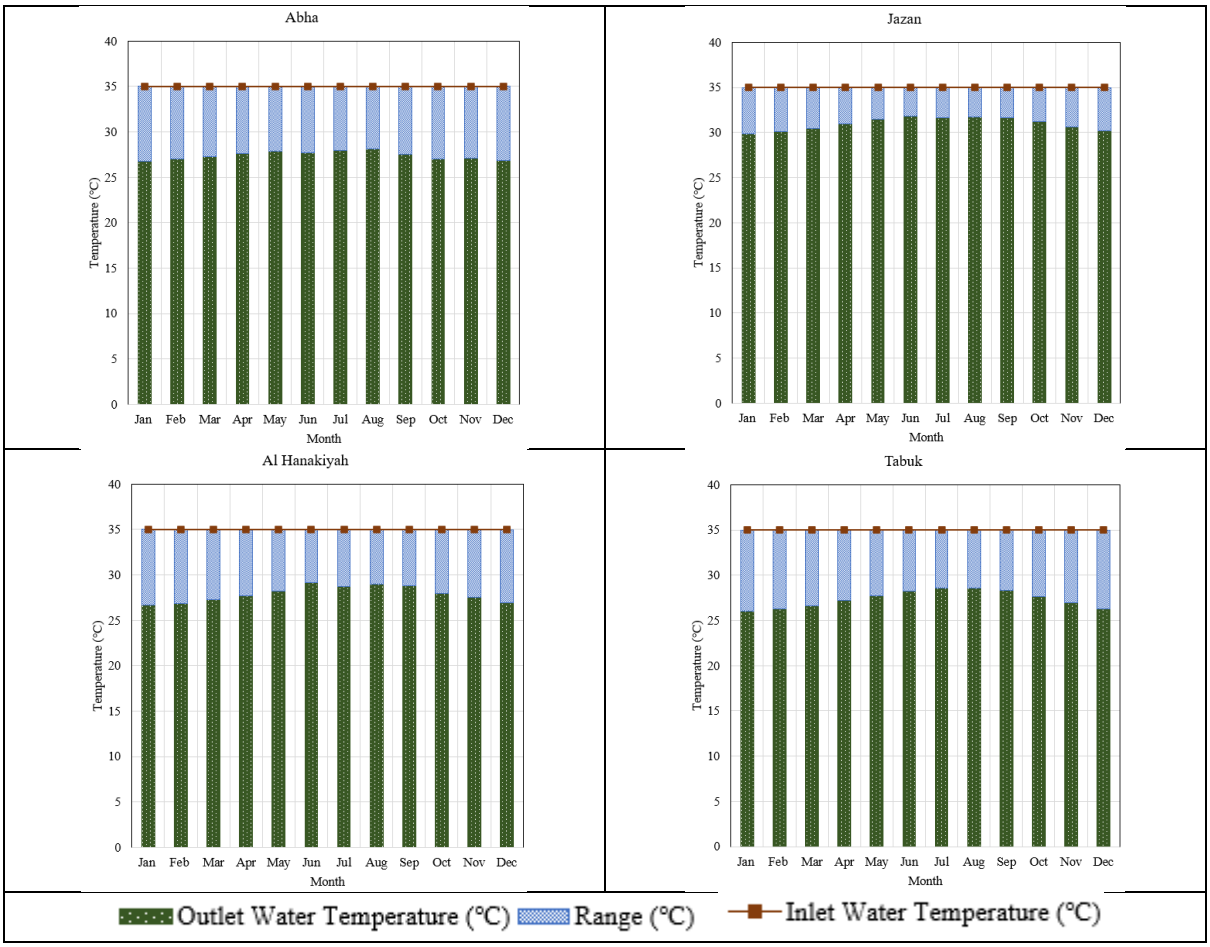

Fig. 8. The Impact of Various Monthly Average Weather Conditions on the Water Temperature Range of the Cooling Tower in 4 Cities in KSA

Fig. 9 provides a comprehensive insight into how diverse monthly average weather conditions impact the cooling capacity of cooling towers across the same four cities.

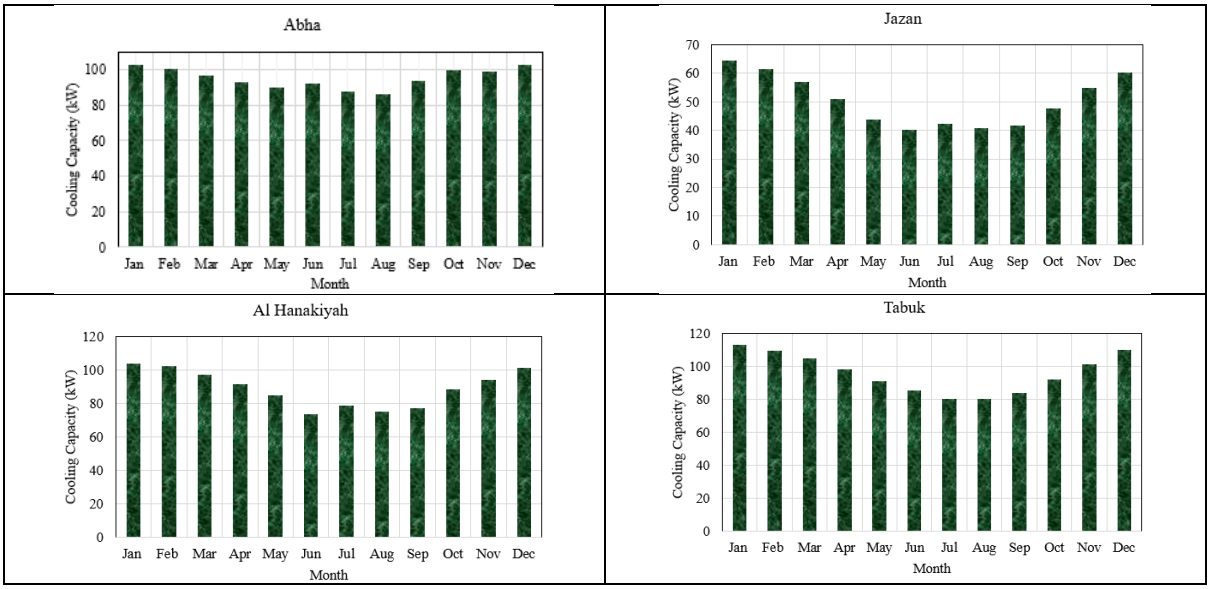

Fig. 9. The Impact of Various Monthly Average Weather Conditions on the Cooling Capacity of the Cooling Tower in 4 Cities in KSA

Throughout the winter season, the cooling tower's ability to cool is at its highest in Abha, Jazan, Al-Hanakiya, and Tabuk, with the most notable effect observed in January. The recorded values for this enhanced cooling capacity are 102.9, 64.5, 103.8, and 112.8 kW, respectively. Transitioning into the summer months, distinct variations come to light. In the cases of Abha and Tabuk, the cooling tower's cooling capacity experienced a decline, reaching its lowest point in August, with measurements of 86.1 kW and 80.08 kW respectively. In contrast, for the cooling towers in Jazan and Al-Hanakiyah, the nadir in cooling capacity is recorded in June, with values of 40.07 kW and 73.6 kW respectively. This discernible trend aligns closely with the impact of temperature range, as evident from the insights provided in Fig. 8. Remarkably, this pattern emphasizes that the cooling tower in Abha excels in its cooling capacity during the warmer months, outperforming its counterparts in other cities, notably Jazan. It's noteworthy that the cooling tower in Jazan experiences its lowest cooling capacity during the summer, further highlighting Abha's advantage in this regard. The magnitude of this cooling capacity discrepancy underscores Abha's cooling tower superiority by a substantial margin of 53.5% compared to the cooling tower's capacity in Jazan. An intriguing observation is that Abha's cooling tower achieves its optimal performance during the summer, owing to its highest temperature range and cooling capacity during this season, particularly in August.

5. CONCLUSIONS

In summary, in this study, we examined the performance of cooling towers across 42 diverse cities in Saudi Arabia. Through the utilization of a developed mathematical model solved with the Engineering Equation Solver (EES), we assessed the cooling tower performance in relation to temperature range and cooling capacity, while giving significant consideration to yearly and monthly average dry-bulb temperatures and relative humidity. Based on the yearly average weather data, the findings showed that the cooling tower exhibits its least efficient operation in Jazan experiencing a temperature range of 4°C with a cooling capacity of 50 kW. Al-Hanakiyah is characterized by high dry-bulb temperatures and low relative humidity. Consequently, the cooling tower in this city exhibits a moderate performance level, encompassing a temperature range of 7.2°C and demonstrating a cooling capacity of approximately 90 kW. On the other hand, the optimal performance of the tower is observed in Tabuk and Abha. Notably, despite different weather conditions in these two cities, the cooling tower's performance remains remarkably comparable. The temperature range in both Tabuk and Abha is approximately 7.61°C, and the cooling capacity achieves a higher level at 95.4 kW. Based on the monthly average weather, the cooling tower

works best in winter, especially in January across all cities. During this time, the cooling tower in Abha, Jazan, Al-Hanakiyah, and Tabuk achieved cooling capacities of 102.9 kW, 64.5 kW, 103.8 kW, and 112.8 kW, respectively. On the other hand, the toughest challenge happens in summer. Compared to the winter, the cooling capacity of the cooling tower in June, in Jazan and Al-Hanakiyah, dropped around 37.8% and 29%, respectively, while in August, the cooling capacity of the cooling tower in Abha and Tabuk experienced reductions of 16.3% and 29%, respectively. Overall, the cooling tower in Abha outperforms its counterpart in Jazan, especially during warmer months. Notably, Abha's cooling tower shows a remarkable 53.5% higher cooling capacity than Jazan's (40.07 kW). This deviation is most prominent in summer when Abha's tower performs exceptionally well, particularly in August.

6. APPENDICES

APPENDIX A

A.1 Correlation Analysis of Manufacturer Data using Linear Regression Method

The experimental data from the manufacturer catalog can be used to develop a correlation using linear regression analysis. This correlation can then be used to directly determine the outlet water temperature, and to validate the results obtained using the model under the same design and operating conditions. Table A1 displays the correlation and the corresponding cooling tower model used, along with the temperatures, mass flowrate, and load ranges analyzed.

Table A1 Correlation Analysis of Manufacturer Data using Linear Regression Method

Correlation	$T_{w,o}^{exp} = 1.39 - 2.37T_{wbi} + 0.338{T_{wbi}}^2 - 0.0059{T_{wbi}}^3 + 1.89T_{wi} + 0.027T_{wi}^2 - 0.0018T_{wi}^3 - 35.149\dot{m}_w - 2.957\dot{m}_w^2 - 0.38\dot{m}_w^3 + 1.57Q_{CC} + 0.00177Q_{CC}^2 + 0.0000325Q_{CC}^3 - 0.24T_{wbi}T_{wi} + 0.0051T_{wbi}T_{wi}^2 - 1.69T_{wbi}\dot{m}_w + 0.061T_{wbi}\dot{m}_w^2 + 0.057T_{wbi}Q_{CC} - 0.0001142T_{wbi}Q_{CC}^2 - 0.00015T_{wbi}^2T_{wi} + 0.031T_{wbi}^2\dot{m}_w - 0.00133T_{wbi}^2Q_{CC} + 3.692T_{wi}\dot{m}_w + 0.033T_{wi}\dot{m}_w^2 - 0.146T_{wi}Q_{CC} + 0.0000159T_{wi}Q_{CC}^2 - 0.058T_{wi}^2\dot{m}_w + 0.0024T_{wi}^2Q_{CC} + 0.056\dot{m}_wQ_{CC} - 0.0027\dot{m}_wQ_{CC}^2 + 0.055\dot{m}_w^2Q_{CC}$
Model	6Z
Temperatures ranges (°C)	$24 \leq T_{w,o} \leq 30$ $29 \leq T_{w,i} \leq 37$
Heat Rejection Range Q_{CC}, (kW)	$27 \leq \dot{Q}_{CC} \leq 114$
Water flowrate range $\left(\frac{kg}{s}\right)$	$1.077 < \dot{m}_w < 4.402$
Size (mm^3)	$1490 \times 686 \times 1750$

ACKNOWLEDGEMENT

The authors of this article highly appreciate and acknowledge the support provided by the DROC and IRC-REPS of King Fahd University of Petroleum & Minerals (KFUPM) through the internal funded project no. INRE2108. The funding support provided by the King Abdullah City for Atomic and Renewable Energy (K. A. CARE) is also acknowledged.

DECLARATION OF INTEREST STATEMENT

The authors declare that they have no known competing financial interests or personal relationships that could have appeared to influence the work reported in this paper. All authors read and approved the final manuscript.

REFERENCE

[1] H. Sayyaadi and M. Nejatolahi, "Multi-objective optimization of a cooling tower assisted vapor compression refrigeration system," International Journal of Refrigeration, vol. 34, no. 1, pp. 243–256, Jan. 2011, doi: 10.1016/j.ijrefrig.2010.07.026.

[2] I. P. Koronaki, E. G. Papoutsis, and V. D. Papaefthimiou, "Thermodynamic modeling and exergy analysis of a solar adsorption cooling system with cooling tower in Mediterranean conditions," Appl Therm Eng, vol. 99, pp. 1027–1038, Apr. 2016, doi: 10.1016/j.applthermaleng.2016.01.151.

[3] W. Peng and O. Karimi Sadaghiani, "Thermodynamic analyses and optimization of an auxiliary heat exchanger equipped with an absorption refrigeration system to increase the cooling capability of Heller cooling tower," Thermal Science and Engineering Progress, vol. 25, p. 101032, Oct. 2021, doi: 10.1016/j.tsep.2021.101032.

[4] A. Ayoub, B. Gjorgiev, and G. Sansavini, "Cooling towers performance in a changing climate: Techno-economic modeling and design optimization," Energy, vol. 160, pp. 1133–1143, Oct. 2018, doi: 10.1016/j.energy.2018.07.080.

[5] J. H. Yu, Z. G. Qu, J. F. Zhang, S. J. Hu, and J. Guan, "Comprehensive coupling model of counter-flow wet cooling tower and its thermal performance

analysis," Energy, vol. 238, p. 121726, Jan. 2022, doi: 10.1016/j.energy.2021.121726.

[6] B. A. Qureshi and S. M. Zubair, "A complete model of wet cooling towers with fouling in fills," Appl Therm Eng, vol. 26, no. 16, pp. 1982–1989, Nov. 2006, doi: 10.1016/j.applthermaleng.2006.01.010.

[7] H. Cui, N. Li, X. Wang, J. Peng, Y. Li, and Z. Wu, "Optimization of reversibly used cooling tower with downward spraying," Energy, vol. 127, pp. 30–43, May 2017, doi: 10.1016/j.energy.2017.03.074.

[8] H.-W. Li, W.-B. Duan, S.-B. Wang, X.-L. Zhang, B. Sun, and W.-P. Hong, "Numerical simulation study on different spray rates of three-area water distribution in wet cooling tower of fossil-fuel power station," Appl Therm Eng, vol. 130, pp. 1558–1567, Feb. 2018, doi: 10.1016/j.applthermaleng.2017.11.107.

[9] K. Singh and R. Das, "A feedback model to predict parameters for controlling the performance of a mechanical draft cooling tower," Appl Therm Eng, vol. 105, pp. 519–530, Jul. 2016, doi: 10.1016/j.applthermaleng.2016.03.030.

[10] Alazazmeh, Ayman Jamal Abdel Majid, and Esmail Mohamed Ali Mokheimer, "Evaporative condenser cooling system.," 9,835,342, Dec. 05, 2017

[11] D. Pandelidis, M. Drąg, P. Drąg, W. Worek, and S. Cetin, "Comparative analysis between traditional and M-Cycle based cooling tower," Int J Heat Mass Transf, vol. 159, p. 120124, Oct. 2020, doi: 10.1016/j.ijheatmasstransfer.2020.120124.

[12] J.-U.-R. Khan, B. A. Qureshi, and S. M. Zubair, "A comprehensive design and performance evaluation study of counter flow wet cooling towers," International Journal of Refrigeration, vol. 27, no. 8, pp. 914–923, Dec. 2004, doi: 10.1016/j.ijrefrig.2004.04.012.

[13] M. Amini, M. Zareh, and S. Maleki, "Thermal performance analysis of mechanical draft cooling tower filled with rotational splash type packing by using nanofluids," Appl Therm Eng, vol. 175, p. 115268, Jul. 2020, doi: 10.1016/j.applthermaleng.2020.115268.

[14] A. Mirabdolah Lavasani, Z. Namdar Baboli, M. Zamanizadeh, and M. Zareh, "Experimental study on the thermal performance of mechanical cooling tower with rotational splash type packing," Energy Convers Manag, vol. 87, pp. 530–538, Nov. 2014, doi: 10.1016/j.enconman.2014.07.036.

[15] D. Lyu, F. Sun, and Y. Zhao, "Impact mechanism of different fill layout patterns on the cooling performance of the wet cooling tower with water collecting devices," Appl Therm Eng, vol. 110, pp. 1389–1400, Jan. 2017, doi: 10.1016/j.applthermaleng.2016.08.190.

[16] M. Rahmati, S. R. Alavi, and M. R. Tavakoli, "Experimental investigation on performance enhancement of forced draft wet cooling towers with special emphasis on the role of stage numbers," Energy Convers Manag, vol. 126, pp. 971–981, Oct. 2016, doi: 10.1016/j.enconman.2016.08.059.

[17] A. C. C. Tomás, S. D. O. Araujo, M. D. Paes, A. R. M. Primo, J. A. P. Da Costa, and A. A. V. Ochoa, "Experimental analysis of the performance of new alternative materials for cooling tower fill," Appl Therm Eng, vol. 144, pp. 444–456, Nov. 2018, doi: 10.1016/j.applthermaleng.2018.08.076.

[18] M. Lucas, J. Ruiz, P. J. Martínez, A. S. Kaiser, A. Viedma, and B. Zamora, "Experimental study on the performance of a mechanical cooling tower fitted with different types of water distribution systems and drift eliminators," Appl Therm Eng, vol. 50, no. 1, pp. 282–292, Jan. 2013, doi: 10.1016/j.applthermaleng.2012.06.030.

[19] P. Shahali, M. Rahmati, S. R. Alavi, and A. Sedaghat, "Experimental study on improving operating conditions of wet cooling towers using various rib numbers of packing," International Journal of Refrigeration, vol. 65, pp. 80–91, May 2016, doi: 10.1016/j.ijrefrig.2015.12.004.

[20] M. Lucas, P. J. Martínez, and A. Viedma, "Experimental study on the thermal performance of a mechanical cooling tower with different drift eliminators," Energy Convers Manag, vol. 50, no. 3, pp. 490–497, Mar. 2009, doi: 10.1016/j.enconman.2008.11.008.

[21] Q. Wei, B. Zhang, K. Liu, X. Du, and X. Meng, "A study of the unfavorable effects of wind on the cooling efficiency of dry cooling towers," Journal of Wind Engineering and Industrial Aerodynamics, vol. 54–55, pp. 633–643, Feb. 1995, doi: 10.1016/0167-6105(94)00078-R.

[22] Z. Zhai and S. Fu, "Improving cooling efficiency of dry-cooling towers under cross-wind conditions by using wind-break methods," Appl Therm Eng,

vol. 26, no. 10, pp. 1008–1017, Jul. 2006, doi: 10.1016/j.applthermaleng.2005.10.016.

[23] K. Wang, F. Sun, Y. Zhao, M. Gao, and L. Ruan, “Experimental research of the guiding channels effect on the thermal performance of wet cooling towers subjected to crosswinds – Air guiding effect on cooling tower,” Appl Therm Eng, vol. 30, no. 5, pp. 533–538, Apr. 2010, doi: 10.1016/j.applthermaleng.2009.10.015.

[24] M. Gao, J. Zou, S. He, and F. Sun, “Thermal performance analysis for high level water collecting wet cooling tower under crosswind conditions,” Appl Therm Eng, vol. 136, pp. 568–575, May 2018, doi: 10.1016/j.applthermaleng.2018.03.043.

[25] X. Chen, F. Sun, Y. Chen, and M. Gao, “Novel method for improving the cooling performance of natural draft wet cooling towers,” Appl Therm Eng, vol. 147, pp. 562–570, Jan. 2019, doi: 10.1016/j.applthermaleng.2018.10.076.

[26] J.-R. Khan and S. M. Zubair, “An Improved Design and Rating Analyses of Counter Flow Wet Cooling Towers,” J Heat Transfer, vol. 123, no. 4, pp. 770–778, Aug. 2001, doi: 10.1115/1.1376395.

[27] B. A. Qureshi and S. M. Zubair, “A unified approach to predict evaporation losses in evaporative heat exchangers,” in International Journal of Refrigeration, Dec. 2011, pp. 1866–1876. doi: 10.1016/j.ijrefrig.2011.06.008.